Protein Partitioning in Two-Phase Aqueous Polymer Systems. 4. Proteins in Solutions of Entangled Polymers

Nicholas L. Abbott,† Daniel Blankschtein,* and T. Alan Hatton

Department of Chemical Engineering, Massachusetts Institute of Technology, Cambridge, Massachusetts 02139

Received April 9, 1992

ABSTRACT: Predictions of scaling arguments for the interactions of globular, hydrophilic proteins with solutions of entangled polymers are compared with measurements of the partitioning of cytochrome-*c* and ribonuclease-a between an entangled (semidilute) aqueous solution of poly(ethylene oxide) (PEO) and a PEO-free aqueous solution using a diffusion cell. The rate of diffusion of PEO of molecular weight 5×10^6 (radius of gyration 1800 Å) through the pores of the membrane (diameter 300 Å) was sufficiently slow as compared to that of the proteins (radius 20 Å) to allow measurement of the equilibrium protein partitioning. Over the range of PEO concentrations 0.08–1.7% w/w, corresponding to $80 < \xi_b < 800$ Å, where ξ_b is the blob size of the semidilute PEO solution, the protein partition coefficients, K_p, were interpreted using the scaling form $\ln K_p = A\phi^\alpha$, where K_p is the ratio of the concentration of protein in the PEO-free and PEO-rich solution compartments and ϕ is the volume fraction of polymer. The experimental value $\alpha = 1.22 \pm 0.06$ was found for both hydrophilic proteins. This exponent lies within the limits $\alpha = 1$ (for $R_p \ll \xi_b$) and $\alpha = {}^9/_4$ (for $R_p \gg \xi_b$) predicted by scaling arguments for the physical exclusion of the proteins from the entangled PEO solution. In view of the similar sizes of ribonuclease-a and cytochrome-*c*, the experimentally determined ratio of the prefactors, $A^{cyto}/A^{ribo} = 1.6 \pm 0.2$, could not be accounted for only on the basis of steric interactions between the proteins and the PEO net. Scaling arguments which incorporated both steric interactions and weak attractive interactions between the proteins and PEO are consistent with the experimentally determined ratio of the prefactors. Charge effects related to the Donnan equilibrium of ions were also investigated by partitioning cytochrome-*c* at pH 7.0 in the presence of the two different salts NaCl and Na_2SO_4 and were determined not to be a dominant contribution to the observed protein partitioning behavior. In particular, the electrical potential difference across the membrane was estimated to be less than 0.2 mV.

1. Introduction

Interest in the partitioning of proteins in two-phase aqueous polymer systems is mainly due to the unique ability of these polymer solutions to provide water-based, yet immiscible, liquid phases for the purification of proteins using liquid–liquid extraction techniques.[1-7] Since each of the two coexisting polymer solution phases contains predominantly water, water-soluble proteins maintain their native conformations and biological activity when purified in these systems. A large number of factors influence protein partitioning, including the types of polymers, their molecular weight and concentration, protein size, conformation and composition, salt type and concentration, and solution pH.[8-12]

In a recent series of papers[13-15] (hereafter referred to as papers 1, 2, and 3) we have reported the influence of the structure of the polymer solution (over length scales corresponding to the sizes of the protein molecules) on the partitioning of proteins in two-phase aqueous polymer systems containing poly(ethylene oxide) (PEO) and dextran.[1] In this two-phase system, the partitioning behavior of a variety of hydrophilic proteins in response to an increase in PEO molecular weight was determined to arise from a transition in the nature of the PEO-rich phase, from a solution containing *individually dispersed PEO coils to a solution of entangled PEO*.[13,15] For proteins in polymer solutions containing *identifiable polymer coils* it was concluded that, in addition to the physical exclusion of the protein by the polymer coils, nonsteric interactions also play a significant role in determining the observed partitioning behavior.[14] In particular, the influence of PEO molecular weight on the equilibrium partitioning behavior of a series of hydrophilic proteins was observed to be consistent with the presence of *both* steric interactions and *weak attractive interactions* between the protein molecules and the polymer coils. Furthermore, the measurement and interpretation of the intensity of neutrons scattered at small angles (SANS) from bovine serum albumin (BSA) (R_p = 35 Å) in aqueous PEO solutions, containing identifiable polymer coils, were also determined to be consistent with weak attractive interactions between BSA and PEO (in addition to the repulsive steric interactions).[15]

While a unified description of the thermodynamic and structural properties of polymer solutions containing identifiable polymer coils and proteins appears to be emerging, the alternative scenario of proteins in polymer solutions containing polymer coils which are extensively entangled has not received sufficient attention. The central aim of the present paper is to provide a description of the interactions of protein molecules and *entangled polymer nets* which complements our earlier descriptions of protein–*polymer coil* interactions. With this aim in mind, results of equilibrium protein partitioning experiments are presented, molecular-level pictures for the interactions of proteins and entangled polymer solutions are proposed, and a complementary scaling-thermodynamic theory is formulated.

Although the partitioning of proteins between entangled polymer solution phases can be studied experimentally using two-phase aqueous polymer systems, several factors introduce ambiguity in the interpretation of such measurements. First, the partitioning of proteins in two-phase aqueous polymer systems reflects the *relative interactions* between the proteins and the *two* coexisting polymer solution phases. Second, the independent control of the polymer concentration in one of the two coexisting phases is not possible since they are coupled through the

* Author to whom all correspondence should be addressed.
† Present address: Department of Chemistry, Harvard University, Cambridge, MA 02138.

0024-9297/92/2225-5192$03.00/0

thermodynamic equilibrium which controls the formation of the two-phase system. To overcome these limitations, we report measurements of the partitioning of proteins between a single entangled polymer solution phase and an aqueous (polymer-free) phase using a diffusion cell (see Figure 1 and section 2C).

The remainder of this paper is organized as follows. In section 2 we discuss experimental considerations, including the construction of a diffusion cell for the measurement of the partitioning behavior of proteins between an entangled polymer solution phase and an aqueous solution. We also discuss precautions taken in our experimental procedure to ensure that *equilibrium* partition coefficients were measured. In section 3 we present results of the experimentally measured partition coefficients of two relatively small hydrophilic proteins, cytochrome-*c* and ribonuclease-a, between an entangled PEO solution and an aqueous solution. Since in two-phase aqueous polymer systems the presence of different salts can have a pronounced effect on the partitioning behavior of proteins which bear net charges, we have also examined the partitioning of cytochrome-*c* in the diffusion cell in the presence of two different salts, NaCl and Na_2SO_4, to assess the importance of salt effects on the diffusion cell measurements. In section 4 we propose molecular-level pictures to describe the interactions of globular proteins and semidilute (entangled) polymer solutions, and in section 5 we predict the associated thermodynamic properties of these solutions. In particular, use is made of scaling concepts from polymer physics[16-20] to predict the protein partitioning behavior associated with each of the proposed molecular-level pictures for the protein–polymer interactions. In section 6 we compare and contrast the experimentally measured and theoretically predicted protein partition coefficients. In so doing we are able to assess the importance of different physical mechanisms in determining the protein partitioning behavior. Finally, in section 6 we also present our concluding remarks.

2. Materials and Experimental Considerations

A. Materials. Poly(ethylene oxide) (PEO) having a nominal molecular weight of 5 000 000 was obtained from Polysciences Inc., Warrington, PA (lot no. 60004). Type V-A, bovine heart cytochrome-*c* and Type I-AS, bovine pancreas ribonuclease-a were purchased from Sigma Chemical Co., St. Louis, MO. All other reagents were of analytical reagent grade, and all solutions were prepared using deionized water which had been conditioned using a Milli-Q ion exchange system (Waters, Milford, MA). Track-etched polycarbonate membranes (which have a narrow distribution of pore sizes) having a 300-Å pore size (lot no. 86B9B55) were obtained from Nucleopore Corp., Pleasanton, CA.

B. Sample Preparation. All samples were prepared in aqueous solutions of 10 mM sodium phosphate buffer to control the pH at 7.0, 1.5 mM sodium azide to prevent bacterial growth in the samples, and either 0.1 M NaCl or 0.05 M Na_2SO_4 to screen electrostatic interactions between the protein molecules. The protein concentrations were less than 1 g/L. The solution pH of 7.0 and low protein concentrations were selected because cytochrome-*c* and ribonuclease-a are not known to self-associate or undergo large conformational changes in the vicinity of this pH or over this range of protein concentrations.[21-28] The PEO solutions were prepared in the buffered salt solution by stirring them for at least 24 h at 25 °C. The polymer solutions were heated briefly (for <1 h) at 45 °C to speed up the dissolution process. No degradation of the polymer under these conditions is expected (PEO of molecular weight 200 000 has been reported to be stable for several days at 50 °C and stable for several weeks at 20 °C).[29,30] This procedure results in aggregate-free aqueous PEO solutions.[15,29,30] All protein solutions were prepared in the same buffer that was used to dissolve PEO and subsequently were prefiltered through a polycarbonate ultrafiltration membrane having a 150-Å pore size (Amicon Co., Danvers, MA). This latter precaution was taken to ensure that any undissolved protein was removed from the solution prior to the experiment.

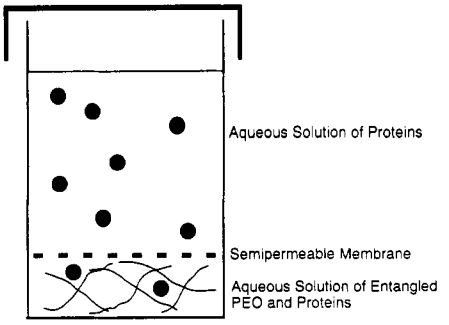

Figure 1. Schematic diagram of the diffusion cell constructed for the measurement of the protein partition coefficients between the top, polymer-free solution and the bottom, entangled polymer solution phase. See section 2C for details.

C. Description of Diffusion Cell. A schematic diagram of the diffusion cell is presented in Figure 1. The diffusion cell is divided into two compartments by a semipermeable membrane having a pore diameter of 300 Å. The bottom compartment, having a volume of approximately 0.8 mL, contained the polymer solution. Since the polymer solution was typically viscous, a magnetic stir bar was used to mix the solution in the lower compartment. The top compartment, having a volume of approximately 7 mL, contained the aqueous protein solution and was maintained free of polymer by the membrane, which, for all practical purposes, was impermeable to the polymer species (the radius of gyration of PEO of molecular weight 5×10^6 is 1900 Å[14]). The protein molecules diffused freely across the membrane and were partitioned between the top and bottom compartments.

The device was constructed by carefully slicing 8-mL plastic sample tubes (Olympic Plastics, Los Angeles, CA) into two sections. The two sections were reattached across a polycarbonate membrane with an epoxy resin (Devcon, Danvers, MA). Care was taken to ensure that only a minimal amount of glue was used and that all the membrane area was available for the diffusion of permeable solutes between the two chambers. Two small holes were made in the bottom section, and the polymer solution (initially free of protein) was injected through the soft plastic tubing into the bottom section at the start of the experiment. Care was taken to remove all air bubbles from the bottom section before it was resealed. The prefiltered protein solution (free of PEO) was poured into the top section of the cell at the beginning of the experiment. All experiments were conducted in a refrigerator at 15 °C. Each cell was discarded after one experiment.

Protein concentrations were determined by measuring the solution absorbance using a Perkin-Elmer Lambda 3B UV–vis spectrophotometer. The concentrations and molecular weight distributions of PEO solutions were determined using a Hewlett-Packard HP-1090 high-pressure liquid chromatograph. The carrier solvent was an aqueous solution of 10 mM sodium phosphate at pH 7.0, 1.5 mM sodium azide, and either 0.1 M NaCl or 0.05 M Na_2SO_4. The chromatograph was operated in a size exclusion mode using a Toya Soda TSK 3000PW, TSK 5000PW, and guard column purchased from Varian Associates (Sunnyvale, CA). The presence of solutes in the eluent phase was detected with a Hewlett-Packard HP-1037A refractive index (RI) detector. The solute concentrations were calculated from the peak areas using the appropriate calibration standards.

D. Partitioning of Proteins into Entangled Polymer Solutions. A control experiment was performed to ensure that in the presence of a PEO-free solution in the bottom compartment the protein was able to diffuse freely across the membrane and establish an equal concentration in the two compartments. This experiment also provided an estimate of the time required to reach equilibrium during the partitioning experiments. It is relevant to mention at this point that a number of larger proteins, including ovalbumin, chymotrypsinogen, and bovine serum albumin, could not be partitioned equally between the two compartments of the cell in a reasonable period of time even in the absence of PEO. Either the time taken to reach equilibrium

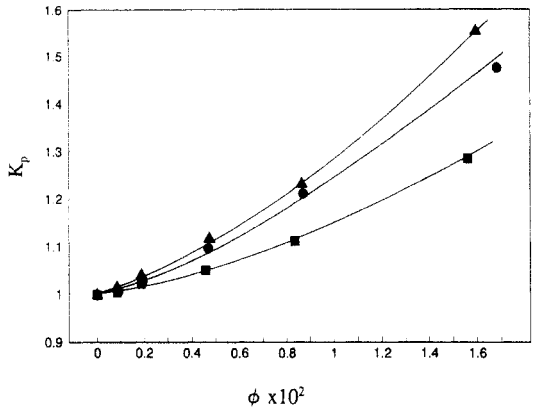

Figure 2. Measured protein partition coefficient, K_p, as a function of PEO volume fraction in the bottom compartment, ϕ: cytochrome-*c* in 0.05 M Na_2SO_4 (▲), cytochrome-*c* in 0.10 M NaCl (●), and ribonuclease-a in 0.05 M Na_2SO_4 (■). All solutions contained 10 mM sodium phosphate buffer (pH 7.0) and 1.5 mM sodium azide.

was prohibitively long or turbidity was detected in the protein solutions before equilibrium was reached, which suggested the formation of aggregates of protein molecules. Only for the two relatively small proteins cytochrome-*c* and ribonuclease-a could the equilibrium be reliably and repeatedly obtained. Multiple samples (typically seven) were prepared for each experiment, and these were examined during the course of the experiment to monitor the approach of the system toward equilibrium. The time taken to reach equilibrium was typically greater than 3 days and less than 1 week (dependent on the polymer concentration). Upon reaching equilibrium, samples were aspirated from the cell with a syringe by piercing a hole in the wall of each compartment. The samples from each cell were analyzed for both polymer and protein concentration.

The concentration of ribonuclease-a was determined by measuring the peak absorbance at 280 nm, and the concentration of cytochrome-*c* was determined by measuring the absorbance at wavelengths of 414 and 549 nm. Since the absorbance spectrum of cytochrome-*c* was found to be sensitive to the oxidation state of the heme moiety, the cytochrome-*c* solutions were reduced with a molar excess of sodium ascorbate to ensure an accurate determination of protein concentrations. All absorbance measurements were referenced to the absorbance of an identical solution without protein.

The polymer concentration was measured using size-exclusion chromatography. The concentrations of polymer in the solutions from both compartments were found to change from their values at the start of the experiment for two reasons: (i) the presence of the polymer in the bottom compartment of the cell produced as osmotic "pumping" of solvent toward that compartment and a concomitant dilution of the concentration of polymer, and (ii) a small flux of polymer was observed to diffuse through the membrane into the top compartment, which also contributed to the dilution of the polymer solution in the bottom compartment and introduced very low concentrations of polymer into the top compartment (see below). Consequently, it was considered very important to monitor accurately the concentration of polymer "introduced" into the (initially polymer-free) top compartment (by the polymer diffusion through the membrane) to ensure that it was always *much less* than the concentration of polymer in the bottom polymer-rich phase.

3. Experimental Results

The partition coefficient of the protein, K_p, is defined as

$$K_p = C_{p,t}/C_{p,b} \quad (1)$$

where $C_{p,t}$ and $C_{p,b}$ are the protein concentrations in the top (PEO-free) and bottom (PEO-rich) compartments, respectively.[1] Figure 2 presents the partition coefficients which were measured as a function of the volume fraction of PEO in the bottom compartment, ϕ, for cytochrome-*c* in buffered salt solutions having concentrations of 0.05 M Na_2SO_4 and 0.1 M NaCl and for ribonuclease-a in a buffered salt solution having a concentration of 0.05 M Na_2SO_4. Figure 2 reveals that as the concentration of PEO is increased, the partition coefficients of both proteins increase. These measurements, which are suggestive of a physical exclusion of the proteins from the volume occupied by PEO, are compared to theoretical predictions in section 6.

Table I
Concentrations of PEO Measured in the Bottom and Top Compartments of the Diffusion Cell after Equilibration of Cytochrome-*c* between the Two Compartments

PEO in top compartment (% w/w)	PEO in bottom compartment (% w/w)
0.00	0.00
0.00	0.08
0.00	0.19
0.00	0.46
0.024	0.85
0.047	1.65

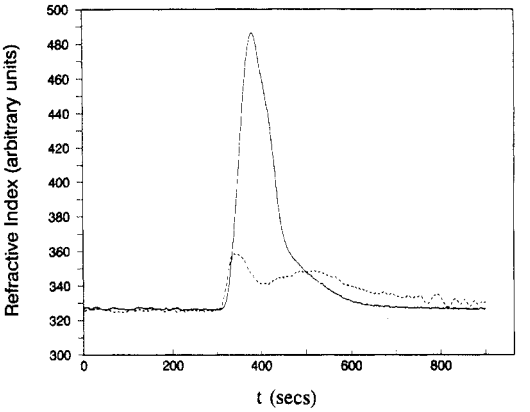

Figure 3. Refractive index (RI) of chromatograph eluent stream as a function of the time elapsed following the injection of samples, *t*, from top (broken line) and bottom (solid line) compartments. Note that the RI unit of measurement for the bottom compartment has been reduced by a factor of 5 for presentation purposes.

To assess the influence of salts on the partition coefficients measured in the diffusion cell, the partitioning of cytochrome-*c* was measured in the presence of NaCl and Na_2SO_4. Inspection of Figure 2 shows that the influence of the different salts is minor as compared to the influence of the PEO concentration (see section 6).

Table I presents the PEO concentrations measured in the top and bottom compartments of the diffusion cell after equilibration of cytochrome-*c* between the two compartments. An examination of Table I shows that, for the sample containing a high initial PEO concentration (1.65% w/w in the bottom compartment), small amounts of PEO (0.047% w/w) are detected in the top (initially polymer-free) compartment after equilibration of the protein concentration. Although some polymer leaked through the membrane, the very low concentration of PEO in the top compartment, as compared to that in the bottom PEO-rich compartment, demonstrates that the flux of PEO through the membrane is sufficiently slow, as compared to the flux of protein, to allow the measurement of an "effective" equilibrium partition coefficient of the protein between the bottom PEO-solution compartment and the top polymer-free solution compartment.

Figure 3 presents results of a HPLC analysis of the two samples reported in the bottom line of Table I (1.65% w/w and 0.047% w/w PEO, bottom and top compartments, respectively). In Figure 3, the HPLC refractive index (RI) detector output (arbitrary units) is plotted as a function of the time following the sample injection. Interestingly, while the refractive index profile (full line) of the solution

from the bottom PEO-rich compartment contains only a single peak, that from the top compartment (dashed line), which contains the PEO which diffused through the membrane, has two large peaks. The presence of the two peaks in the RI profile is suggestive of a bimodal polymer molecular weight distribution. The peak at $t \simeq 500$ s in the chromatogram corresponding to the PEO solution sample from the top compartment is a fraction of PEO with a low molecular weight. This peak presumably arises due to the more rapid diffusion of the smaller PEO coils through the membrane pores (as compared to the higher molecular weight PEO molecules). Although the molecular weight distributions of PEO are rather different in the two solution compartments, for our purposes, the polymer concentration in the top compartment was maintained sufficiently low such that it could be neglected when interpreting the protein partitioning results. However, we wish to emphasize that if the polymer concentration in the top compartment becomes comparable to that in the bottom compartment, the different molecular weight distributions could become a very important consideration when interpreting the protein partitioning behavior.

4. Physical Pictures for the Interactions of Proteins in Solutions of Entangled Polymers

To elucidate the nature of the interactions between PEO and proteins in aqueous solution, the length scales which characterize the aqueous PEO solution and which are used to describe the interactions between PEO and proteins must be identified. At polymer concentrations greater than c^* (where c^* is a threshold polymer concentration characteristic of the region where the extensive overlap of polymer coils begins to occur), the polymer coils overlap and are entangled to form a polymer solution web or mesh.[16] Within this mesh, the identities of the individual polymer coils are lost and *all* thermodynamic properties of the solution are independent of the molecular weight of the polymer coils. The characteristic length scale of the polymer solution is the size (blob size) of the polymer web, ξ_b, which is also a measure of the range of correlations between polymer segments in the solution and which scales with polymer volume fraction, ϕ, as[16]

$$\xi_b \sim a\phi^{-3/4} \tag{2}$$

For aqueous (D_2O) solutions of PEO, small-angle neutron scattering (SANS) measurements have determined $a \simeq 4$ Å, which is consistent with the known flexibility of PEO.[15,29]

In Figure 4, we show two possible scenarios for the interactions of globular protein molecules with entangled polymers in solution. These scenarios reflect differences in the relative sizes of the polymer solution blob, ξ_b, and the protein, R_p, in addition to the strength of the attractive interactions between the polymer segments and the protein molecules, which is characterized by ϵ (measured in units of kT). More specifically, ϵ is the energy change associated with bringing a single polymer segment from a solvated environment to the protein surface. When $R_p \ll \xi_b$ and only steric interactions occur between the protein and the polymer segments, the protein behavior will be similar to that of an inert solvent species, capable of diffusing relatively unhindered through the polymer net (Figure 4a). While the protein is unaware of the blob size of the polymer solution, it can interact simultaneously with a group of correlated polymer segments (belonging to the same strand of polymer) within a volume that is of the order of the volume of the protein.

A rather different situation prevails when the protein size is much larger than the polymer blob size, that is, when $R_p \gg \xi_b$. In this case, repulsive excluded-volume interactions between polymer strands and the impenetrable protein surface will cause a depletion of the polymer segments near the protein surface (Figure 4b). Because the polymer segments communicate the presence of the protein surface over distances corresponding to the correlation length of the polymer solution, the length scale of the depletion layer will be of order ξ_b. In this case, since the radius of the protein is large compared to the correlation length of the polymer solution, the curvature of the protein surface does not play a dominant role in determining the interactions of the protein and the polymer mesh (other than to define the surface area of the protein).

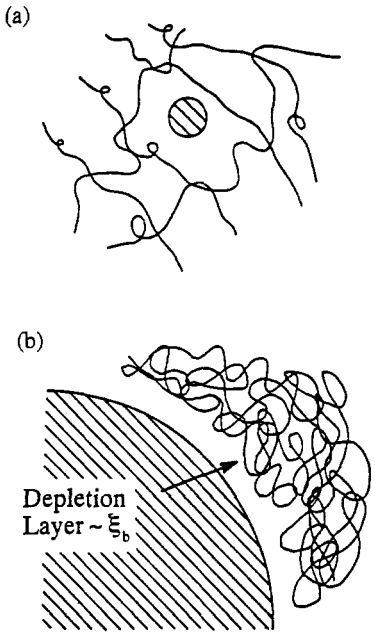

Figure 4. Two possible scenarios for the interactions of globular proteins and high molecular weight polymers: (a) $R_p \ll \xi_b$ and very weak attraction or no attraction between the polymer and the protein; (b) $R_p \gg \xi_b$ and very weak attraction or no attraction between the polymer and the protein. For details see sections 4 and 5.

In keeping with the developments of paper 1, one can also imagine scenarios where there are both steric and weak (perturbative) attractive interactions between the protein molecules and the polymer segments.[13] Under conditions such that the attraction is sufficiently weak (which is defined more precisely in section 5), the structures of the solutions, as presented in Figure 4, are preserved.

In contrast to the case of weak attractions, the presence of a stronger attraction between the protein molecules and the polymer segments will promote the "decoration" of the protein surface with an adsorbed layer of polymer. For polymer solution conditions where the polymer blob size greatly exceeds the size of the protein ($R_p \ll \xi_b$), the proteins may adsorb onto the polymer net like beads on a necklace.[29] In the alternative limit, $R_p \gg \xi_b$, the polymer strands will adsorb to the surface of the protein, just as they would do at a macroscopic and planar surface. Because a number of theoretical attempts have been previously reported to describe the free-energy change associated with the complexation of spheres and flexible polymers[17-20] and because we have not performed experimental measurements for proteins which partition into the PEO-rich compartment (which is a necessary condition for complexation to occur), here, we do not further treat this regime of behavior.

In the following section, we examine the consequences of the scenarios depicted in Figure 4 on the thermodynamic

properties of the solutions. In particular, we focus on predicting the partitioning of proteins between an entangled polymer solution and an aqueous (polymer-free) solution. We emphasize the physical scenarios depicted in Figure 4 because they are consistent with experimental measurements as well as with our earlier descriptions of the interactions of similar proteins with PEO solutions containing identifiable polymer coils.[13-15]

5. Scaling-Thermodynamic Theory

A. Statistical-Thermodynamic Framework. In the limit of vanishing protein concentration, interactions between protein molecules are very weak, and the equilibrium partition coefficient of the protein is simply related to the free-energy change *of the system* associated with the transfer of a protein molecule from the top (PEO-free) compartment into the bottom (PEO-rich) compartment of the diffusion cell. Accordingly, the partition coefficient of the protein, K_p, can be expressed as[13]

$$\ln K_p = \ln\left(\frac{C_{p,t}}{C_{p,b}}\right) = \left(\frac{\mu^\circ_{p,b}(T,P+\Pi,\phi) - \mu^\circ_{p,t}(T,P)}{kT}\right) + \left(\frac{z_p e(\psi_b - \psi_t)}{kT}\right) \quad (3)$$

where $\mu^\circ_{p,i}$ is the standard-state chemical potential of the protein in compartment i (top (t) or bottom (b)), Π is the osmotic pressure of the polymer solution in the bottom compartment, z_p is the net charge of the protein, e is the elementary charge, ψ_i is the electrical potential in compartment i, k is the Boltzmann constant, and T is the absolute temperature. The physical interpretation of the protein standard-state chemical potential is the free-energy change upon taking a protein from a polymer-free solvent phase at temperature T and pressure P and introducing it into a solution having a composition, temperature, and pressure corresponding to the conditions in either the top or the bottom compartment of the diffusion cell. The macroscopic electrical potential term in eq 3 (the last term) accounts for the Donnan-type potential associated with the diffusional equilibrium of charged species (proteins and electrolytes) between the two compartments of the diffusion cell.[1,26,31,32]

The physical origin of the potential difference $\psi_b - \psi_t$ in eq 3 is the interactions of the salt ions, water, and PEO, and consequently this contribution is ion specific.[1,26,31,32] In view of the relatively small influence that Na_2SO_4 and NaCl have on the partitioning of cytochrome-*c*, as reported in Figure 2 and discussed in section 3, it appears that the contribution of the last term in eq 3 to K_p is not dominant at these low PEO concentrations. Accordingly, for the range of PEO concentrations considered in Table I, eq 3 simplifies to

$$\ln K_p \approx \left(\frac{\mu^\circ_{p,b}(T,P+\Pi,\phi) - \mu^\circ_{p,t}(T,P)}{kT}\right) \quad (4)$$

The term $\mu^\circ_{p,b}(T,P+\Pi,\phi) - \mu^\circ_{p,t}(T,P)$ in eq 4 corresponds to the free-energy change accompanying a reversible isothermal process where a protein is transferred from a pure solvent phase at pressure P to a polymer solution phase having a polymer concentration ϕ at pressure $P + \Pi$. We consider $\mu^\circ_{p,b}(T,P+\Pi,\phi) - \mu^\circ_{p,t}(T,P)$ to be divided into the three contributions ΔG_p, ΔG_2, and ΔG^{att}. Accompanying the introduction of the protein into the polymer solution, interactions between proteins and polymer segments (which can be steric and energetic) constrain the translational freedom of the protein, and as a result an entropic penalty is incurred. The corresponding free-energy change is denoted as ΔG_p. The second contribution, which mirrors ΔG_p, is due to the influence of the same interactions (between the protein and the polymer segments) on the configurational and translational freedom of the polymers. This contribution is denoted as ΔG_2. Clearly, while these two contributions to $\mu^\circ_{p,b}(T,P+\Pi,\phi) - \mu^\circ_{p,t}(T,P)$ are coupled through the nature of the interactions between the protein and the polymer segments, it turns out (as shown below) that, depending on the solution conditions, only one of these two contributions is significant. The third term, ΔG^{att}, accounts for the contribution of the energetic interactions between the protein and the polymer segments to the free-energy change. In keeping with the division of the protein standard-state chemical potential into these three contributions, we evaluate the protein partition coefficients using

$$\ln K_p \approx \left(\frac{\Delta G_p + \Delta G_2 + \Delta G^{att}}{kT}\right) \quad (5)$$

B. Figure 4a: $R_p \ll \xi_b$, $\epsilon = 0$. Figure 4a corresponds to solution conditions where the protein size, R_p, is much smaller than the blob size of the polymer solution, ξ_b, and the only interaction between the polymer segments and the protein occurs because they cannot occupy the same physical space ($\Delta G^{att} = 0$). Statistical-thermodynamic considerations equate the *total* (volume) fraction of the solution excluded to the protein, u_p, with $\Delta G_p/kT$; that is, $\Delta G_p/kT = u_p$.[33] Depending upon the relative sizes of the protein, R_p, and the polymer persistence length, b, the functional dependence of u_p on R_p can vary. Here we focus on the case relevant to the interactions of PEO and globular protein molecules, where the size of the protein is large compared to the persistence length of the polymer chain. When the flexibility of the polymer chain occurs at the length scale of a monomer, a, the interactions between the polymer segments and the protein molecule are not independent. That is, a significant probability exists, which increases with the protein size, that two or more polymer segments belonging to the same polymer strand will interact simultaneously with the protein. Specifically, the protein will interact with the strands of polymer which have sizes similar to R_p. The number of polymer segments, n_a, within a strand of polymer having size, $R_a \sim a n_a^{3/5}$, comparable to the size of the protein, is given by

$$n_a \sim (R_p/a)^{5/3} \quad (6)$$

Since, by definition, these "protein-sized blobs" interact independently with a protein molecule, the total volume excluded from the protein per protein-sized blob is of order R_p^3. The number of protein-sized blobs in solution (per unit volume of solution), N_a/V, is required to evaluate the total (volume) fraction of the solution which is excluded from the protein by the blobs, that is, $u_p \sim (N_a/V)R_p^3$. Since the molecular volume of a blob is of the order of $n_a a^3$, it follows that $N_a/V \sim \phi/(n_a a^3)$. Using $\Delta G_p/kT = u_p$ and eq 6 we obtain

$$\frac{\Delta G_p}{kT} \sim \frac{N_a R_p^3}{V} \sim \frac{\phi R_p^3}{a^3 n_a} \sim \phi\left(\frac{R_p}{a}\right)^{4/3}, \quad a \ll R_p \ll \xi_b \quad (7)$$

Equation 7 can be compared to the simpler case where the polymer chain is rigid on the length scale of the protein molecule ($a \ll R_p \ll b$). In this case, all polymer segments interact independently with the protein molecule, and, therefore, the volume fraction of solution excluded from the protein can be estimated by considering the interactions of a very long rod (the polymer chain) and a sphere (the protein), that is, $u_p = \phi(R_p/a)^2$. The exponent of R_p

in eq 7, $^4/_3$, which is smaller than the corresponding exponent in the case of the rigid polymer chain, 2, reflects the fact that when the polymer chain becomes flexible on a length scale comparable to the protein size, the protein will interact simultaneously, on average, with several polymer segments. Note that a form similar to eq 7 has been derived previously by de Gennes using a slightly different argument.[18]

To predict the protein partition coefficient using eq 5, we also require an estimate of ΔG_2. This can be obtained by evaluating the $P-V$ type work required to introduce a protein into the polymer solution by displacing a volume U_2 against the solution osmotic pressure, that is, $\Delta G_2 = \Pi U_2$, where U_2 is the volume of the solution that is excluded from the polymer by the protein. While the configurational freedom of the polymer chains is reduced in the vicinity of the protein surface (which results in the exclusion of the polymer from that vicinity), at distances beyond (order) R_p from the protein surface, the polymer can no longer "feel" the presence of the protein and thus experiences the freedom of the bulk solution. Consequently, the polymer is excluded from a volume of the solution of order R_p^3. Scaling relations for the osmotic pressure of the polymer solution, Π, which account for the existence of correlations between polymer segments, predict that the osmotic pressure scales as[16]

$$\Pi \sim kT/\xi_b^3 \tag{8}$$

Using eq 8 for the osmotic pressure of the polymer solution and $U_2 \sim R_p^3$, ΔG_2 can be evaluated as

$$\frac{\Delta G_2}{kT} = \frac{\Pi U_2}{kT} \sim \left(\frac{R_p}{\xi_b}\right)^3 \tag{9}$$

In the limit, $R_p/\xi_b \ll 1$, this contribution is negligible as compared to ΔG_p given in eq 7 (which, using eq 2, is of order $(R_p/\xi_b)^{4/3}$). Using the result $\Delta G_p \gg \Delta G_2$ and inserting eq 7 into eq 5 along with $\Delta G^{att} = 0$, the protein partition coefficient, in the limit $R_p \ll \xi_b$, is given by

$$\ln K_p \sim \phi(R_p/a)^{4/3}, \quad a \ll R_p \ll \xi_b \tag{10}$$

C. Figure 4a: $R_p \ll \xi_b$, $0 < \epsilon \ll 1$. In view of the significant role that attractive protein–polymer interactions (in addition to steric interactions) play in determining the thermodynamic properties of proteins in solutions which contain identifiable PEO coils,[13-15] we have examined the influence of such weak attractions on the partition coefficients measured in the diffusion cell experiments with entangled PEO solutions. To evaluate the influence of the attractions, we have made two simplifying assumptions, both of which are consistent with those made previously when treating the interactions of proteins and PEO solutions containing identifiable polymer coils:[13-15] (i) attractive interactions between polymer segments and protein molecules are short-ranged (with a range of the order of the polymer segment size), and (ii) the distribution of polymer segments in the vicinity of the protein molecule is not perturbed significantly by the presence of weak attractive interactions. With these two assumptions in mind, the influence of the perturbative weak attractive interaction on ΔG^{att} can be estimated from the number of polymer segments, N^*, found, on average, within a distance of order a from the protein surface. That is

$$\Delta G^{att}/kT = -\epsilon N^* \tag{11}$$

For the case of a protein that is large compared to the persistence length of the polymer chain ($R_p \gg b$), we consider the interaction of N_a/V "protein-sized polymer blobs" (each containing n_a polymer segments) with the protein molecule (see eq 6 and the accompanying text). This physical situation is analogous to the interaction of N_a/V polymer *coils* per unit volume (each having n_a statistical segments) with protein molecules which was considered in paper 1. That is, for a solution of N_a/V polymer coils which interact with the protein with an energy ϵ per polymer-segment contact, the influence of an attractive interaction on ΔG^{att} can be written as

$$\frac{\Delta G^{att}}{kT} \sim -\epsilon \frac{N_a}{V} R_p^2 a n_a^{2/5} \tag{12}$$

Equation 12 was derived in paper 1 by considering a balance of two opposing effects.[13] First, when a protein and a blob interact, the density of polymer segments that is "felt" by the protein molecule scales with the density of polymer segments, ρ_a, within a polymer coil having its unperturbed average configuration, $\rho_a \sim n_a/R_g^3$, which decreases as $a^{-3}n_a^{-4/5}$ with increasing polymer size.[16] Second, with each interaction, the number of polymer segments interacting with the protein will be proportional to the product of the available surface area of the protein, R_p^2, and to the range of the interaction, a, as well as to the product of the "surface area" of the blob, defined by $R_a^2 \sim a^2 n_a^{6/5}$, and a. Finally, eq 12 also accounts for the probability of an interaction occurring between a protein molecule and a polymer blob, which is proportional to the number of protein-sized polymer blobs (per unit volume) in solution, N_a/V. To estimate ΔG^{att} we substitute $N_a/V = \phi/n_a a^3$ and eq 6 into eq 12 to obtain

$$\frac{\Delta G^{att}}{kT} \sim -\epsilon\phi\left(\frac{R_p}{a}\right) \tag{13}$$

It is relevant to compare eq 13 to an equivalent equation which can be obtained using a different form for N^*, derived previously by de Gennes,[18] namely

$$\frac{\Delta G_p^{att}}{kT} \sim -\epsilon\phi\left(\frac{R_p}{a}\right)^{1/3} \tag{14}$$

The difference between eqs 14 and 13 appears because in the evaluation of eq 13 we have attempted to include the fact that when a protein-sized polymer blob and a protein molecule interact, the strength of the interaction will depend on the number of contacts with the polymer segments. As mentioned above, we have predicted that the number of such contacts scales as $n_a^{6/5-4/5} = n_a^{2/5}$. If this contribution is omitted, then eq 13 becomes identical to eq 14.

Substituting eqs 9 and 13 into eq 5, along with the condition $\Delta G_p \gg \Delta G_2$, yields

$$\ln K_p \sim \phi\left(\frac{R_p}{a}\right)^{4/3}\left[1 - k_1\epsilon\left(\frac{a}{R_p}\right)^{1/3}\right], \quad a \ll R_p \ll \xi_b \tag{15}$$

where k_1 is a numerical constant of order unity.

D. Figure 4b: $R_p \gg \xi_b$, $\epsilon = 0$. For the scenario where the size of the protein, R_p, is large compared to the size of the polymer blob, ξ_b, the interactions between the protein molecule and the polymer net are determined by the relative sizes of the protein and the polymer correlation length. In this case, we will show that the dominant contribution to the protein partition coefficient in eq 5 is the term ΔG_2. This contribution can be evaluated as the reversible isothermal work done to exclude the polymer from the protein volume and the polymer depletion layer at the protein surface, denoted as U_2, against the osmotic pressure of the polymer solution.[18] That is

$$\Delta G_2 = \Pi U_2 \sim \Pi(R_p + \xi_b)^3 \tag{16}$$

where the depletion of the polymer extends a distance ξ_b from the surface of the protein (see section 4). Using eq 8 for Π in eq 16 and the condition $R_p \gg \xi_b$, the following scaling form for ΔG_2 is obtained:[17]

$$\frac{\Delta G_2}{kT} \sim \left(\frac{R_p}{\xi_b}\right)^3 \sim \phi^{9/4}\left(\frac{R_p}{a}\right)^3, \quad a \ll \xi_b \ll R_p \quad (17)$$

where eq 2 has been used to relate ξ_b to ϕ.

To estimate the magnitude of ΔG_2 in the limit $R_p \gg \xi_b$, it is useful to reconsider the evaluation of ΔG_p in the limit $R_p \ll \xi_b$. Equation 7 predicts that in the limit $R_p \ll \xi_b$, where polymer segments interact with the protein independently, $\Delta G_p \sim \phi$. On the other hand, as the ratio R_p/ξ_b increases, polymer segments will simultaneously exclude the protein, and thus the volume excluded (from the protein) *per polymer* will decrease. Therefore, eq 7 also forms an upper bound on the magnitude of ΔG_p for $R_p \gg \xi_b$. Using eq 2, eq 7 can be rewritten in the following form:

$$\frac{\Delta G_p}{kT} \sim \left(\frac{R_p}{\xi_b}\right)^{4/3} \quad (18)$$

Comparing eq 18 with eq 17 shows that, in the limit $R_p \gg \xi_b$, ΔG_2 is much larger than ΔG_p. Accordingly, in the limit $R_p \gg \xi_b$, the partition coefficient of the protein can be written as

$$\ln K_p \sim \phi^{9/4}\left(\frac{R_p}{a}\right)^3, \quad a \ll \xi_b \ll R_p \quad (19)$$

E. Figure 4b: $R_p \gg \xi_b$, $0 < \epsilon \ll 1$. In the spirit of previous scaling arguments,[16,18] we have proposed the following extension of eq 19 to account for the influence of weak attractive interactions between the polymer segments and the protein surface. Specifically, the attractive interactions between the polymer segments and the protein surface are insufficient to deform the polymer strands extensively in the vicinity of the protein (from the case $\epsilon = 0$). Provided that $0 < \epsilon \ll 1$, this scenario appears reasonable (unless $n_s\epsilon > 1$, where n_s is the number of surface contacts). Under these conditions, using the equality of the osmotic pressures in the bulk and at the surface, as suggested by de Gennes,[16] the concentration of polymer in the bulk, ϕ, can be related to the concentration of polymer at the surface of the protein, ϕ_s, by the relation

$$\phi_s \sim \phi^{9/4} \quad (20)$$

If the introduction of the very weak attractive interaction between the polymer segments and the protein does not significantly perturb ϕ_s, substituting $N^* = (R_p/a)^2\phi_s$ into eq 11 leads to the following form for ΔG^{att}:

$$\frac{\Delta G^{att}}{kT} \sim -\epsilon\phi^{9/4}\left(\frac{R_p}{a}\right)^2 \quad (21)$$

In eq 21 the number of contacts between the protein molecule and the polymer segments is proportional to the surface area of the protein, R_p^2. The form of the protein partition coefficient which incorporates both repulsive steric and weak attractive interactions between the protein molecule and the polymer net is obtained by summing eqs 19 and 21, that is

$$\ln K_p \sim \phi^{9/4}\left(\frac{R_p}{a}\right)^3\left(1 - k_2\epsilon\left(\frac{a}{R_p}\right)\right), \quad a \ll \xi_b \ll R_p \quad (22)$$

where k_2 is a numerical constant of order unity.

6. Results and Discussion

First, we compare the theoretical predictions of the protein partition coefficients reported in section 5 with the experimental measurements. The experimentally measured K_p vs ϕ curves presented in Figure 2 have been rationalized according to the general scaling law dependence of $\ln K_p$ on ϕ derived in section 5. Specifically, we take (see eqs 15 and 22)

$$\ln K_p = A\phi^\alpha \quad (23)$$

For the three sets of data in Figure 2, corresponding to cytochrome-*c* in buffered NaCl (0.1 M) and Na_2SO_4 (0.05 M) solutions and to ribonuclease-a in buffered Na_2SO_4 (0.05 M) solutions, the exponents, α, and intercepts, $\ln A$, are presented in Table II (see also Figure 5). An examination of Table II reveals that (1) the same exponent $\alpha = 1.22 \pm 0.06$ (within the statistical uncertainty) was determined for cytochrome-*c* and ribonuclease-a in 0.05 M Na_2SO_4 and for cytochrome-*c* in the presence of the two different salts (NaCl and Na_2SO_4) and (2) the intercept determined for cytochrome-*c* ($\ln A = 4.2 \pm 0.1$) differs from that determined for ribonuclease-a ($\ln A = 3.6 \pm 0.1$). We first discuss the value of the exponent, α, and then the values of the prefactor, A.

Corresponding to the scenarios depicted in Figure 4, eqs 10 and 19 predict α values of 1 and $^9/_4$, respectively. The experimentally determined value of 1.22 appears closer to the exponent $\alpha = 1$ predicted for Figure 4a (see eq 10), where $R_p \ll \xi_b$. The effective spherical sizes (see Table III) of cytochrome-*c* and ribonuclease-a are both approximately 20 Å, and, over the range of PEO concentrations studied, the accompanying variation in the blob size was from 80 to 800 Å. Clearly, this is consistent with the constraint $R_p \ll \xi_b$ or, at least, $R_p < \xi_b$. Finally, it is noteworthy that, while the experimentally determined exponent, $\alpha = 1.22$, lies between the limits $\alpha = 1$ and α

Table II
Exponents and Prefactors Obtained from a Comparison of $\ln K_p = A\phi^\alpha$ with the Experimental Data Presented in Figure 2

protein	salt	exponent, α	prefactor, $\ln A$
cytochrome-*c*	0.10 M NaCl	1.20 ± 0.04	4.17 ± 0.09
cytochrome-*c*	0.05 M Na_2SO_4	1.26 ± 0.03	4.29 ± 0.07
ribonuclease-a	0.05 M Na_2SO_4	1.22 ± 0.04	3.64 ± 0.10

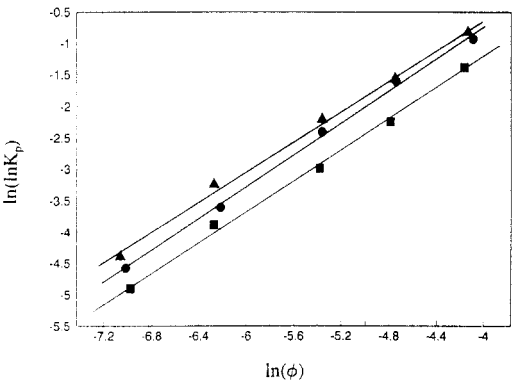

Figure 5. Double logarithm of the protein partition coefficient, $\ln(\ln K_p)$, as a function of the logarithm of the volume fraction of PEO in the bottom compartment, $\ln \phi$: cytochrome-*c* in 0.05 M Na_2SO_4 (▲), cytochrome-*c* in 0.10 M NaCl (●), and ribonuclease-a in 0.05 M Na_2SO_4 (■). All solutions contained 10 mM sodium phosphate buffer (pH 7.0) and 1.5 mM sodium azide.

Table III
Physical Properties of Cytochrome-*c* and Ribonuclease-a

physical property	cytochrome-*c*[a]	ribonuclease-a[b]
molecular weight	12 384	13 690
diffusion coefficient (cm^2/s)	10.1×10^{-7}	10.7×10^{-7}
dimensions (Å^3)	15 × 17 × 17	19 × 14 × 11
hydrodynamic radius (Å)	21	20

[a] References 42 and 44. [b] Reference 43.

$= {}^9/_4$, there was no indication of a crossover between these two exponents over the range of PEO concentrations investigated (which exceeded an order of magnitude variation).

While the values of the prefactor, A, determined from the two cytochrome-c partitioning experiments (see Table II) are the same ($\ln A^{cyto} = 4.2 \pm 0.1$), the value of A determined for ribonuclease-a ($\ln A^{ribo} = 3.6 \pm 0.1$) is significantly smaller. In accordance with the above discussion on the dependence of K_p on ϕ in Figure 4a, where $R_p \ll \xi_b$ and only steric interactions operate between the protein and the polymer segments, the difference in the prefactors is given by (see eq 10)

$$\ln A^{ribo} - \ln A^{cyto} = \frac{4}{3} \ln \left(\frac{R_p^{ribo}}{R_p^{cyto}} \right) \tag{24}$$

Using the experimental values for $\ln A^{ribo}$ and $\ln A^{cyto}$ from Table II, the ratio of the protein sizes is predicted to be

$$R_p^{cyto}/R_p^{ribo} = 1.6 \tag{25}$$

In Table III a comparison of some relevant physical properties of cytochrome-c and ribonuclease-a is presented. An examination of Table III shows that these proteins have similar physical dimensions. In addition, using the diffusion coefficient data, also presented in Table III, along with the Stokes–Einstein equation,[33] the ratio of the effective spherical hydrodynamic radii is 1.06 and, therefore, differs significantly from that predicted by eq 25. This suggests that, in addition to steric interactions between the proteins and the PEO segments, other interactions may be responsible for the differences in the partitioning behaviors of the two proteins.

The combined influence of repulsive steric and weak attractive interactions on the protein partition coefficient (for $R_p \ll \xi_b$) is described by eq 15. Since the influence of the attractions is only perturbative, the term in brackets in eq 15 should be very close to unity and can therefore be rewritten approximately as

$$\ln K_p \sim \phi \left(\frac{R_p}{a} \right)^{4/3} \exp\left(-k_1 \epsilon \left(\frac{a}{R_p} \right)^{1/3} \right) \tag{26}$$

This equation predicts that the difference in the A values for cytochrome-c and ribonuclease-a (assuming $R_p^{ribo} \simeq R_p^{cyto} = R_p$) is given by

$$\ln A^{ribo} - \ln A^{cyto} = -k_1(\epsilon^{ribo} - \epsilon^{cyto}) \left(\frac{a}{R_p} \right)^{1/3} \tag{27}$$

Taking $R_p = 20$ Å and $a = 4$ Å for PEO, eq 27 indicates that, to account for the observed value of $\ln A^{ribo} - \ln A^{cyto}$, the difference in the attractive interaction energies should satisfy $k_1(\epsilon^{ribo} - \epsilon^{cyto}) \simeq 1$. One possible difference between the two proteins, which may account for these different interactions energies, is the presence of the heme moiety on cytochrome-c. This suggestion is supported by the different partitioning behaviors of heme proteins and nonheme proteins in two-phase aqueous polymer systems containing PEO. Specifically, in two-phase aqueous dextran–PEO systems at pHs corresponding to the isoelectric points of each protein, the partition coefficient of ribonuclease-a ($K_p = 0.8$) is higher than that of cytochrome-c ($K_p = 0.5$), indicating the preferred partitioning of ribonuclease-a toward the PEO-rich phase, as compared to cytochrome-c.[24]

Our measurements of the partitioning behavior of cytochrome-c in the diffusion cell suggest that the influence of salts on the observed partitioning behavior is very small. This observation constrasts with experimental measurements in two-phase aqueous PEO–dextran systems, where the substitution of NaCl by Na_2SO_4 is found to have a profound effect on the observed protein partitioning.[24] To reconcile this difference a few comments are in order. First, it is relevant to note that in two-phase aqueous PEO–dextran systems the magnitude of the salt effect, traditionally characterized by a bulk electrical potential difference, $\Delta\psi$, between the two-phases, correlates linearly with the difference in the concentration of PEO in each of the coexisting phases.[31,32] In two-phase aqueous PEO–dextran systems, this difference is typically 10% w/w PEO, and the corresponding $\Delta\psi$ is about 1–2 mV. In the diffusion cell experiments, the PEO concentrations are an order of magnitude smaller, typically about 1% w/w or less (see Table I), and thus the anticipated electrical effects are expected to be less pronounced. Indeed, one can make an estimate of the strength of $\Delta\psi$ from the partition coefficients measured for cytochrome-c in the presence of the two different salts. The influence of the salt on the partition coefficient of the protein can be expressed as (see eq 3)

$$\ln K_p^{salt} = \frac{z_p e \delta\psi}{kT} \tag{28}$$

At pH 7.0, the net charge of cytochrome-c is $z_p = +6$,[34,35] and using the partition coefficient data in Figure 2 for cytochrome-c at $\phi = 0.016$, namely, $K_p^{NaCl} = 1.56$ and $K_p^{Na_2SO_4} = 1.47$, the difference in the electrical potential, $\Delta\psi^{Na_2SO_4} - \Delta\psi^{NaCl}$, calculated using eq 28, is approximately 0.2 mV. This value, which is an order of magnitude less than that typically encountered in two-phase aqueous PEO–dextran systems, is consistent with the fact that we are dealing with PEO concentrations which are concomitantly smaller. While one could further investigate the influence of the salts by measuring the partition coefficient as a function of pH, as has been done in two-phase aqueous polymer systems,[27] the interpretation of these measurements is complicated by conformational changes of the protein which, in general, accompany changes in solution pH.

In comparing the partitioning behaviors of proteins in two-phase aqueous polymer systems and in the diffusion cell, it is interesting to note another difference which appears when comparing eq 4 and the thermodynamic framework of paper 1.[13] In the two-phase aqueous polymer systems considered in paper 1, proteins are partitioned across a *planar liquid–liquid interface* between the two coexisting polymer solution phases which are *at the same pressure*. In contrast, in the diffusion cell experiment, the mechanical membrane which separates the top and bottom compartments *can support a pressure difference*. This pressure difference, which corresponds to the osmotic pressure of the polymer solution, Π, can lead to significant differences in the predicted protein partitioning behaviors. For example, we can compare eq 19 with the prediction for the partitioning of proteins between two phases at constant pressure, such as the partitioning of proteins in two-phase aqueous polymer systems containing entangled polymer solution phases. In the latter case, the work done in transferring a protein molecule from one phase to the other corresponds to the work done against the osmotic pressure in forming (only) the depletion layer about the protein. Specifically, the volume of the protein is not included in the excluded volume since the same pressure is exerted on this volume in both phases. Accordingly, from a simple modification of eq 16, where now $U_2 \sim$

$R_p^2\xi_b$, ln K_p is predicted to have the form

$$\ln K_p \sim \phi^{3/2}(R_p/a)^2, \quad a \ll \xi_b \ll R_p \qquad (29)$$

A comparison of eqs 29 and 19 shows the rather different exponents that relate the protein partition coefficient to ϕ and R_p for the two subtly different experimental situations.

Finally, we mention that a number of investigations exist on the hindered diffusion of globular colloids through polymer networks.[36-41] Indeed, just as thermodynamic properties are influenced by the relative sizes of the globular species and the polymer solution correlation length (in addition to their energetic interactions with the net), the hindered diffusion of a globular species through the net is influenced by similar factors. Although in this paper we have considered issues related to the equilibrium properties of proteins in entangled polymer solutions, the study of the hindered diffusion of proteins through the entangled polymer solution complements this report.

In conclusion, we have reported experimental measurements of the partitioning behavior of two small proteins (cytochrome-*c* and ribonuclease-a) between entangled aqueous solutions of PEO and PEO-free aqueous solutions using a diffusion cell. The rate of diffusion of the high molecular weight PEO through the dividing membrane was sufficiently slow as compared to that of the proteins that equilibrium protein partitioning results could be obtained. Comparison of the experimental measurements to predictions obtained using scaling arguments, which were developed to describe the interactions of proteins and entangled polymers, suggests that steric interactions between the proteins and PEO are important in determining the protein partition behavior. In addition, however, in view of the similar sizes of the proteins that were partitioned and yet their different partitioning behaviors, we conclude that, in addition to steric interactions, other types of interactions occur between the proteins and PEO. Specifically, the observed differences in the partitioning behaviors of cytochrome-*c* and ribonuclease-a are consistent with scaling arguments which include both steric interactions and weak attractive interactions between the proteins and PEO. Since a similar conclusion was reached for proteins in solutions containing singly-dispersed polymer coils (dilute solutions),[13-15] a unifying picture seems to be emerging for *both* dilute and entangled PEO solutions that rationalizes protein partitioning behavior in terms of both steric and weak attractive interactions between the proteins and PEO.

Acknowledgment. Support for this work was provided by the National Science Foundation (NSF) through the Biotechnology Process Engineering Center at MIT under Grant CDR-88-03014 and a NSF Presidential Young Investigator (PYI) Award to D.B. and by the Whitaker Foundation. In addition, D.B. was supported through NSF Grant DMR-84-18718, administered by the Center for Materials Science and Engineering at MIT. D.B. is also grateful for the support by the Texaco–Mangelsdorf Career Development Professorship at MIT as well as to BASF, British Petroleum America, Exxon, Kodak, and Unilever for providing PYI matching funds. N.L.A. is grateful to the George Murray Scholarship Fund of the University of Adelaide, Adelaide, Australia, for financial support.

References and Notes

(1) Albertsson, P. A. *Partition of Cell Particles and Macromolecules*; Wiley: New York, 1986.
(2) Walter, H.; Brooks, D. E.; Fisher, D., Eds. *Partitioning in Aqueous Two-Phase Systems*; Academic Press: New York, 1985.
(3) Kula, M.-R.; Kroner, K. H.; Hustedt, H. *Adv. Biochem. Eng.* **1982**, *24*, 73.
(4) Hustedt, H.; Kroner, K. H.; Stach, W.; Kula, M.-R. *Biotechnol. Bioeng.* **1978**, *20*, 1989.
(5) Kula, M.-R.; Kroner, K. H.; Hustedt, H.; Schutte, H. *Ann. N.Y. Acad. Sci.* **1981**, *341*.
(6) Tjerneld, F.; Berner, S.; Cajarville, A.; Johansson, G. *Enzyme Microb. Technol.* **1986**, *8*, 417.
(7) Birkenmeier, G.; Kopperschlager, G.; Albertsson, P. A.; Johansson, G.; Tjerneld, F.; Akerlund, H. E.; Berner, S.; Wickstroem, H. *J. Biotechnol.* **1987**, *5*, 115.
(8) Walter, H.; Johansson, G. *Anal. Biochem.* **1986**, *155*, 215.
(9) Carlson, A. *Sep. Sci. Technol.* **1988**, *23*, 785.
(10) Baskir, J. N.; Hatton, T. A.; Suter, U. W. *Biotechnol. Bioeng.* **1989**, *34*, 541.
(11) Abbott, N. L.; Blankschtein, D.; Hatton, T. A. *Bioseparation* **1990**, *1*, 191.
(12) Walter, H.; Johansson, G.; Brooks, D. E. *Anal. Biochem.*, in press.
(13) Abbott, N. L.; Blankschtein, D.; Hatton, T. A. *Macromolecules* **1991**, *24*, 4334.
(14) Abbott, N. L.; Blankschtein, D.; Hatton, T. A. *Macromolecules* **1992**, *25*, 3917.
(15) Abbott, N. L.; Blankschtein, D.; Hatton, T. A. *Macromolecules* **1992**, *25*, 3932.
(16) de Gennes, P.-G. *Scaling Concepts in Polymer Physics*; Cornell University Press: Ithaca (NY) and London, 1988.
(17) Alexander, S. *J. Phys. (Paris)* **1977**, *38*, 977.
(18) de Gennes, P.-G. *Co. R. Hebd. Seances Acad. Sci.* **1979**, *288*, 359.
(19) Pincus, P. A.; Sandroff, C. J.; Witten, T. A. *J. Phys. (Paris)* **1984**, *45*, 725.
(20) Marques, C. M.; Joanny, J. F. *J. Phys. (Paris)* **1988**, *49*, 1103.
(21) Sasakawa, S.; Walter, H. *Nature* **1970**, *223*, 329.
(22) Sasakawa, S.; Walter, H. *Biochemistry* **1972**, *11*, 2760.
(23) Walter, H.; Sasakawa, S.; Albertsson, P. A. *Biochemistry* **1972**, *11*, 3880.
(24) Zaslavsky, B. Y.; Mestechkina, N. M.; Rogozhin, S. V. *J. Chromatogr.* **1983**, *260*, 329.
(25) Albertsson, P.-A.; Cajarville, A.; Brooks, D. E.; Tjerneld, F. *Biochim. Biophys. Acta* **1987**, *926*, 87.
(26) Johansson, G. *J. Chromatogr.* **1985**, *322*, 425.
(27) Diamond, A. D.; Hsu, J. T. *Biotechnol. Bioeng.* **1989**, *34*, 1000.
(28) Diamond, A. D.; Hsu, J. T. *AIChE J.* **1990**, *36*, 1017.
(29) Cabane, B.; Duplessix, R. *J. Phys. (Paris)* **1987**, *48*, 651.
(30) Cabane, B.; Duplessix, R. *J. Phys. (Paris)* **1982**, *43*, 1529.
(31) Bamberger, S.; Seaman, G. V. F.; Brown, J. A.; Brooks, D. E. *J. Colloid Interface Sci.* **1984**, *99*, 187.
(32) Brooks, D. E.; Sharp, K.; Bamberger, S.; Tamblyn, C. H.; Seaman, G. V. F.; Walter, H. *J. Colloid Interface Sci.* **1984**, *102*, 1.
(33) Tanford, C. *Physical Chemistry of Macromolecules*; Wiley: New York, 1961.
(34) Theoreu, H.; Akesson, A. *J. Am. Chem. Soc.* **1941**, *63*, 1812.
(35) Wu, C. F.; Chen, H. S. *J. Chem. Phys.* **1987**, *87*, 6199.
(36) Lin, T. H.; Phillies, G. D. J. *J. Phys. Chem.* **1982**, *86*, 4073.
(37) Lin, T. H.; Phillies, G. D. J. *J. Colloid Interface Sci.* **1984**, *100*, 82.
(38) Lin, T. H.; Phillies, G. D. J. *Macromolecules* **1984**, *17*, 1686.
(39) Ullmann, G. S.; Ullmann, K.; Linder, R. M.; Phillies, G. D. J. *J. Phys. Chem.* **1985**, *89*, 692.
(40) Phillies, G. D. J.; Ullmann, G. S.; Ullmann, K.; Lin, T. H. *J. Chem. Phys.* **1985**, *82*, 5242.
(41) Brown, W.; Rymden, R. *Macromolecules* **1986**, *19*, 2942.
(42) Dickerson, R. E.; Takano, T.; Eisenberg, D.; Kallai, O. B.; Samson, L.; Cooper, A.; Margoliash, E. *J. Biol. Chem.* **1971**, *246*, 1511.
(43) Squire, P. G.; Himmel, M. E. *Arch. Biochem. Biophys.* **1979**, *196*, 165.
(44) Cohn, E. J.; Edsall, J. T. *Proteins, Amino Acids and Peptides*; Reinhold: New York, 1943.

Registry No. PEO, 25322-68-3; NaCl, 7647-14-5; Na_2SO_4, 7757-82-6; cytochrome-*c*, 9007-43-6; ribonuclease-a, 9001-99-4.